



Original paper

Removal of sulfate from Gamasiab river water samples by using natural nano-Clinoptilolite

Amir Hossein Salimi, Sayed Farhad Mousavi, Saeed Farzin*

Department of Water Engineering and Hydraulic Structures, Faculty of Civil Engineering, Semnan University, Semnan, Iran.

ARTICLE INFO

Article history:

Received 22 February 2019

Received in revised form 30 March 2019

Accepted 15 April 2019

Keywords:

Gamasiab river

Natural nano-clinoptilolite

Sulfate ion

Adsorption

Design expert software

ABSTRACT

Rivers serve as one of the main sources of water supply. Human activities, salts in the soil and rocks and urban runoffs, as well as air contaminants, lead to contamination of river water. In this research, Gamasiab river, which is the upstream of Karkheh river, was selected as a case study. Sixteen stations were selected along this river to determine the sulfate content of water samples. Samples were taken from these stations according to the guidelines (ISO 5667-5, 1991). The samples were then transferred to laboratory and were filtered using nanoparticles of natural clinoptilolite. The X-Ray Diffraction (XRD), Transmission Electron Microscopy (TEM) and Fourier-Transform Infrared Spectroscopy (FTIR) images were taken to determine the properties of the adsorbents. The images indicated that the selected methods for preparation of the nanoparticles were correctly implemented. After examining the filtered samples, the adsorption efficiency was 95% for clinoptilolite. Whatman filter paper 42 was used for desorption of the natural nano-clinoptilolite. Adsorption isotherm of the natural clinoptilolite was Freundlich with a determination coefficient of $R^2=0.918$. By using Design Expert software and assumption of two pH factors and adsorbent to contaminant ratios (D/C), optimum adsorption points were found and theoretical adsorption values were calculated as well. Results showed that the optimum adsorption points for clinoptilolite were $\text{pH} = 9.51$ $(\text{mg})_{\text{adsorbent}}/(\text{mg/L})_{\text{initial}}$ and $\text{D/C}=18.91$ $(\text{mg})_{\text{adsorbent}}/(\text{mg/L})_{\text{initial}}$. Comparison of the adsorbent function indicated that clinoptilolite had good performance in removal of sulfate ion from river water samples.

©2019 Razi University-All rights reserved.

1. Introduction

Water scarcity and its availability has been always one of the major problems in agricultural sector (Salimi et al. 2018). In addition, rivers have always been considered as the most important source of water supply. This is why most of the old civilizations were established in the vicinity of the rivers. River water can be contaminated by various factors. One of the known sources of water pollution is sulfates. These pollutants are usually found in nature in places with sedimentary rocks or near the oil wells. These pollutants can also be found in citrus gardens and agricultural fields due to the use of fertilizers containing sulfate, or wastewater from some factories. Like other minerals, sulfates can cause flaky layers in water pipes, may cause undesirable taste, eventually leads to diarrhea in humans and domestic livestock, and even cause problems in washing clothes (Heizer et al. 1997). Due to these effects, the need to eliminate sulfates from water resources has always been one of the human concerns.

In the current century, there is a need for technological innovations for seamless management of water supply. Among the existing technologies, nanotechnology has the potential to achieve this goal. This technology helps to improve the efficiency of wastewater treatment and unconventional sources of water, and leads to clean and safe water. (Hu et al. 2013). By studying earlier researches, it was found that many nanoparticles and nanotubes have been used to purify specific pollutants in some river water samples in the laboratory. For example, copper, lead, nickel and cadmium ions can be separated from aqueous solutions using silica porous nanoparticles (Ezzeddine

et al. 2015), or removing lead, copper and silver ions (Zaho et al. 2015). In addition, by using silver nanoparticles, heavy metals can be removed from water samples containing river sediments (Tao et al. 2016). All these cases are examples of the use of natural nanoparticles in the purification of target pollutants from water solutions.

But, it is possible to use more complex structures in nanomaterials for improving the purification capacity and increasing the treatment efficiency for extensive range of pollutants. Typically, using iron nanoparticles that have been synthesized from different leaf extracts of plants (which are eco-friendly solutions) can be used to treat domestic wastewater (Devatha et al. 2016). Other uses of nanostructures include the use of magnetic carbon nanotubes in removal of nitrate pollutant (Alimohammadi et al. 2016). It is also possible to open up a new horizon in water purification using microporous organic polymers (Li et al. 2017). New research has shown that selenium can be effectively removed from aqueous solutions using hematite-coated magnetic nanoparticles (Ma et al. 2018).

Earlier researches can easily highlight the importance of water and continuous efforts to develop new water sources. The use of nanoparticles, especially natural nanoparticles, is one of the options for providing fresh water through treatment of contaminated water due to ease of access as well as being cheap.

2. Materials and methods

2.1. Features of the study area

*Corresponding author Email: saeed.farzin@semnan.ac.ir

The study area is located at 47° 21' to 47° 54' east longitude and 34° 16' to 35° 34' north latitude (Fig. 1), Kermanshah province, Iran. The length of the studied river (Gamasiab) in this area is 74.7 km. This river originates from Sang Surakh springs, which are located 21 km southeast of Nahavand city, Hamadan province. The flow direction in the river is from east to west and northwest to southwest. Along the route of the river, Dinevar Ab joins it. The river reach is divided into two sections. The first section is from entrance point of the river to Kermanshah province to the intersection with Dinevar Ab river (34.4 km). The second section is from this junction down to the intersection with Gharahsu River and formation of the Seymareh river (40.3 km). Sixteen stations were selected for sampling water from the Gamasiab river.

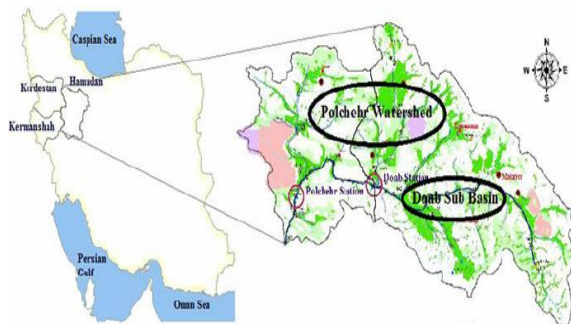


Fig. 1. Location map of Gamasiab river.

EPA standards for drinking water have two types of classification (primary standards and secondary standards). Sulfate is in the category of secondary standards and its maximum level (SMCL) in drinking water is 250 mg/L (Biswas, 1997). After determining the initial sulfate content of the samples, which were taken from the river, they were filtered by using the adsorbents. The natural clinoptilolite particles' diameter that were used in this study was less than 100 nm. Also, the carbon nanotube was coated by iron compound (FeCl₂. 4H₂O) from the Arak mines, Iran. In order to determine the concentration of the river-water pollutants, spectrophotometer (Hach Company DR 5000), for determining the pH, pH-meter model 713, for weighing the materials, electronic balance KEB5003 with a precision of ± 0.0001 g, for creation of nitrogen atmosphere to coat iron compounds with nanotubes, a nitrogen capsule made in Iran, for drying the samples, an oven (BM55E Model), made in Iran, for FTIR images, FT_IR Cary604 model made in USA, sieve (mesh 400) made in Iran, and for XRD pictures, Xpertpro model of the Panalytical Company of the Netherlands, were used.

2.2. Sampling and laboratory procedures

Gamasiab river plays a significant role in water supply of western provinces of Iran. Along this river, 16 stations were selected for qualitative sampling and analysis. Sampling from Gamasiab river was done according to ISO 5667-5, 1991 standards. After sampling, 90 ml water samples were poured in clean plastic containers and placed in an insulated casing with dimensions of to be transferred to the lab. Sulfate concentration of the samples was measured in the laboratory according to the standard methods (SMAWW, 1998) using a spectrophotometer (DR 5000 model) and sulfate detector kit (purchased from Mehregan Sanat Ab Co.). The kit had barium chloride and citric acid as stabilizer. After transferring the samples to 10 ml cells, the detector was added to the samples until the solution was completed. Then, they were rested for 5 minutes. Finally, after cleaning each cell, they were placed in the device and the read-button was pressed. To determine the sulfate concentration, the device was set to 450 nm. The efficiency of adsorbents was calculated using equation below.

$$\text{Removal \%} = (q_i - q_t) / q_i \quad (1)$$

where, q_i is initial concentration of contaminant and q_t is contaminant concentration after treatment.

2.3. Preparation of nanoparticles

The zeolitic material with particle size range from 50 nm to 100 nm, was supplied by Afrand Tooska Co, (Negin Powder Co., Ltd.) in

Isfahan province, Iran. It was converted to nanoparticles by using a planetary ball-mill (PM100, Retsch Corporation, 600 rpm, 6 h). As a result of this process, the stone size reached less than 100 nm. Then, a certain amount of clinoptilolite sample was poured into 100 ml of water and incubated at room temperature (25 °C) for two hours. The lid of the container was closed and kept in the room for 24 hours. The solution was then passed through a filter paper. The obtained powder was heated at 90 °C in distilled water on a magnetic stirrer for 8 h to remove any water-soluble and magnetic impurities (3 times).

2.4. Designing the experiment and Design Expert software

In this research, response surface methodology (RSM) has been used to design the experiments. RSM is one of the optimization methods that models the issues using a set of mathematical and statistical techniques, and not only reduces costly simulation performance, but also natural process of optimization, which is often nonlinear, is predicted. RSM techniques can be used in different ways depending on their application in the design of the test, including central combination method (CCD), D-Optimal and Box-Behnken (Box and Draper, 2007). Design Expert software package is a statistical package that was presented by Stat-Ease in 1988 for design of the tests. Using this software, you can make comparative tests, screening, mixing designs, etc. Design Expert provides expert matrix of test matrix for screening up to 50 factors. The statistical significance of these factors was analyzed by analysis of variance (ANOVA) (Montgomery, 2004). Due to limitations in the laboratory conditions, samples were simulated for pH and adsorbent to contaminant ratios (D/C) in Design Expert software.

2.5. Isotherm of adsorption

Isotherm is the most important parameter in design of adsorption systems and describes the relationship between the adsorbent concentration and adsorption capacity of the adsorbent. Two common isotherms are Langmuir and Freundlich isotherms. The Langmuir isotherm assumes valence points on the adsorbent surface. So, the absorbed layer will be as thick as a molecule (Redlich and Peterson, 1959). Langmuir's linear equation is expressed as:

$$\frac{C_e}{q_m} + \frac{1}{K_L \cdot q_m} = \frac{C_e}{q_e} \quad (2)$$

where, C_e is equilibrium concentration of the material in the solution (mg/L), q_e is the amount of material adsorbed in terms of solid content (mg/g), K_L is Langmuir coefficient, and q_m is maximum adsorption in the Langmuir model. The Langmuir adsorption index is obtained as follows.

$$R_L = \frac{1}{1 + K_L \cdot C_0} \quad (3)$$

where, C_0 is maximum initial concentration (mg/L), K_L is Langmuir constant, and R_L is Langmuir index. In the above equation, if $R_L > 1$, the model is undesirable, $R_L = 0$ is for irreversible model, $R_L = 1$ is for linear model and if $0 < R_L < 1$ the model is desirable. The multilayer adsorption isotherm is expressed by Freundlich model. The adsorption regions are not at the same level and have different absorption capacities. Freundlich's linear equation is usually expressed as follows.

$$\log q_e = \log K_f + \left(\frac{1}{n}\right) \log C_e \quad (4)$$

where, q_e is concentration of the adsorbed ion (mg/L), C_e is concentration of pollutant (mg/L) and K_f and n are Freundlich adsorption coefficients (L/mg). According to the correlation coefficient R^2 , the closer it is to 1, the isotherm is closer to the results of the lab. In order to find the best kinetics and adsorption isotherm, test data were analyzed using RMSE and R^2 statistical criteria (Ho et al. 2004).

3. Results and discussion

3.1. Identification of adsorbents

To identify the properties of the adsorbents, XRD, FTIR and TEM images were prepared for clinoptilolite, as shown in Figs. 2 to 4, respectively. In Fig. 2, XRD for clinoptilolite is shown in the angle of $10^\circ - 40^\circ = 2\theta$. In the XRD data, the characteristic lines at grade 2θ are 10° , 11.4° , 17.4° , 23° , 26° , 28.2° , 30° and 32° , similar to the

clinoptilolite XRD data corresponding to JCPDS 38-0237 (Rabo, 1976). XRD data proved that the mineral stone used includes clinoptilolite as the most important component as well as 4.5 % of quartz and 9.2 % cristobalite. The clinoptilolite FTIR spectrum up to 4000 cm⁻¹ is shown in Fig. 3. It should be noted that the in-situ measurement method is based on the pure powder of KBr under nitrogen flow. TEM images of clinoptilolite are shown in Fig. 4. In this Fig., the particle dispersion is indicated as well as the mean particle size (about 50 nm).

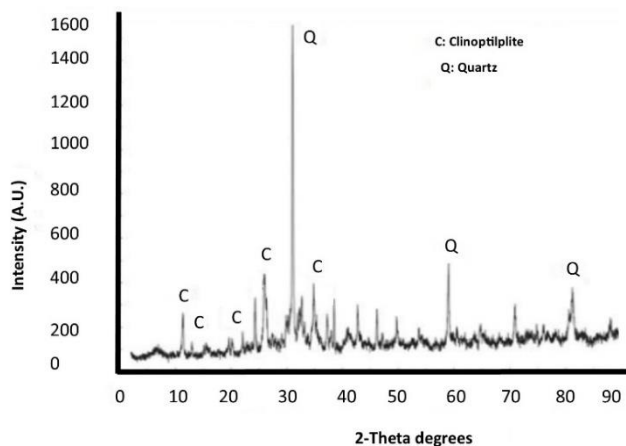


Fig. 2. XRD of clinoptilolite.

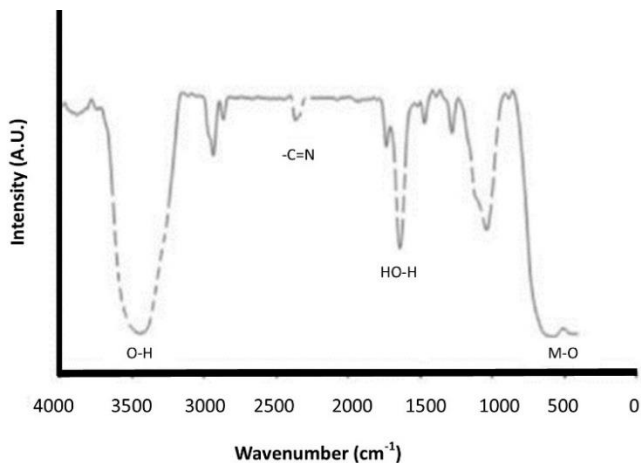


Fig. 3. FTIR of clinoptilolite.

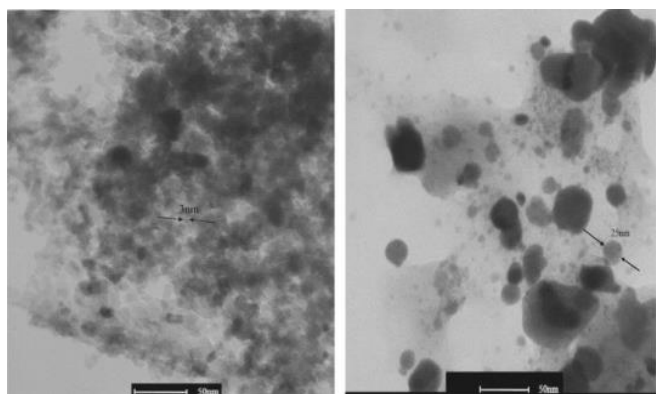


Fig. 4. TEM of clinoptilolite.

3.2. Equilibrium time, sulfate changes in water samples and adsorption efficiency

By adding adsorbents to water samples and examining the samples after 0.5, 1, 6, 12, 24 and 48 hours, it was tried to calculate the equilibrium time. For this purpose, as shown in Fig. 5, at each step after the application of the adsorbent, the amount of contaminant and consequently, the percentage of adsorption, was calculated by

equation (1). According to the data shown in Fig. 5 and using equation 1, sulfate adsorption efficiency for clinoptilolite was calculated to be 91.5 %. As it is known, after 0.5 hr, about 78 % of the sulfate was adsorbed by the clinoptilolite. With the advancement of the experiment, in the next steps, this amount increased to the extent that it reached about 91 % after 48 hr. After 48 hr, less than 3 % of the change in efficiency occurred. Therefore, the adsorbent equilibrium time was considered to be 24 hr after adsorption. Results of the sulfate-concentration changes, before and after the use of adsorbent, in the water samples from the 16 selected stations are shown in Fig. 6.

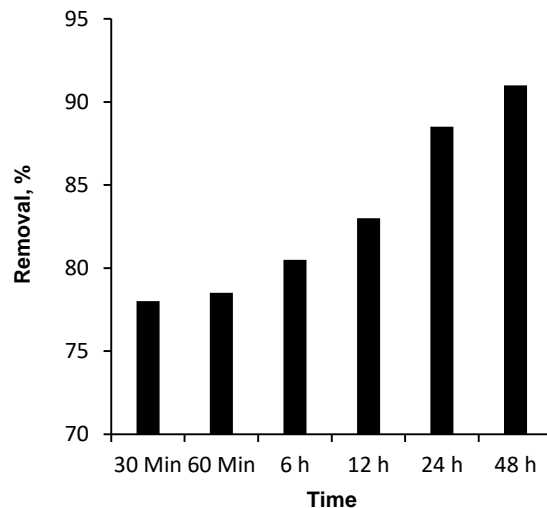


Fig. 5. Equilibrium time vs. removal percentage.

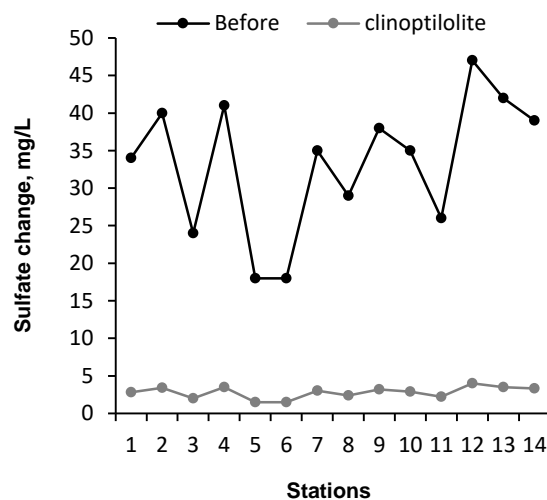


Fig. 6. Sulfate changes before and after the use of adsorbent.

To find the optimal conditions for using the adsorbents, expert design of the experiments was used. Among the RSM, the CCD is the most important and comprehensive. In this study, this method was considered for accurate evaluation of the two independent variables. The ratio of adsorbent concentration (mg/L) to initial concentration of the contaminant (D/C) ((mg)_{adsorbent}/(mg/l)_{initial}) and pH were selected as control variables. The design consists of a complete factorial at two levels (2²=8), four star points and a central point. In addition, three replications of the experiment were carried out at the central point to evaluate the net error between each test. For clinoptilolite, pH and D/C were measured in ranges of 3 to 12 and 5 to 100 (Table 1). In order to study the parameters, their interaction and their squared errors on the removal of sulfate by clinoptilolite, the results of laboratory analysis for different removal percentages were analyzed by ANOVA. Table 2 shows the ANOVA results for the removal of sulfate by clinoptilolite. Combination of estimates for variables and results of ANOVA shows that polynomial models were statistically significant. The models for refined sulfate with clinoptilolite are shown in the following.

$$\text{Removal, \%} = +16.07674 + 17.18832 \text{ pH} - 0.92092 * \text{D/C} + 0.069708 * \text{pH} * \text{D/C} - 0.97346 * \text{pH}^2 - 3.37950\text{E-}004 * \text{D/C}^2$$

Table 1. Factors and levels for CCD study for clinoptilolite.

Level	pH, X1	D/C, X2
-α	3	5
-1	4.32	18.91
0	7.5	52.5
1	10.68	86.09
	12	100

By using this equation, the relative error percentage, prediction of the percentage of optimal removal, RSM graph and level curve were

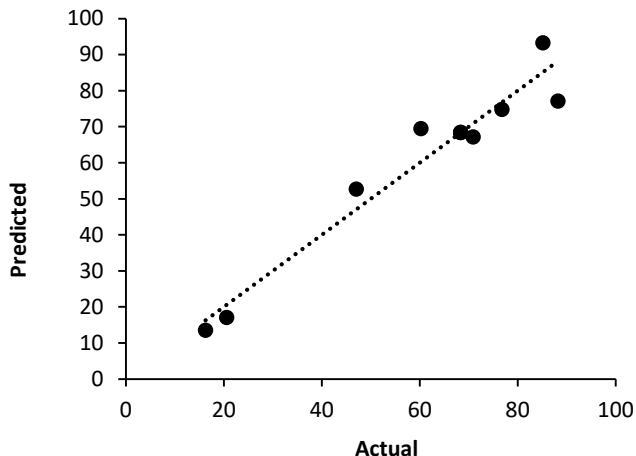


Fig. 7. Actual and predicted data for clinoptilolite.

extracted. The experimental results were compared with the theoretical model derived from equation 5. The mean error for clinoptilolite was 4.18 %. Regarding the relative error and the existence of two independent parameters and a dependent parameter in the equation, the relative error percentage is acceptable. Fig. 7 shows the trend of real and predicted data changes. This figure shows that as experimental values get closer to the X=Y line, the model is more accurately able to estimate the experimental results. Simultaneous effect of efficiency (desirability), pH and D/C changes in adsorbent for clinoptilolite is depicted in Fig. 8. As this figure indicates, the highest levels of efficiency have occurred in the alkaline region. In addition, increasing D/C, reduced the removal efficiency of clinoptilolite.

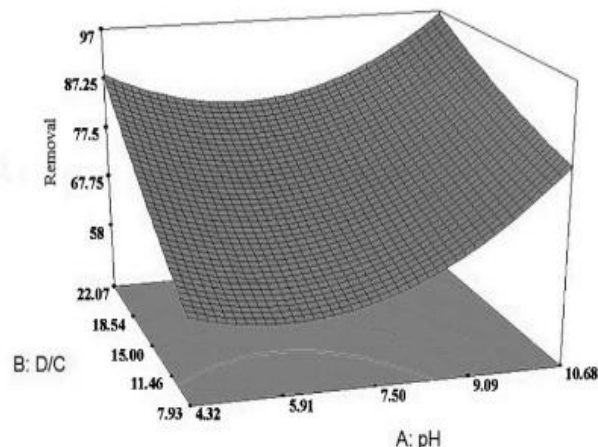


Fig. 8. Contour plot describing the response surface of clinoptilolite's desirability as a function of pH and D/C.

Table 2. ANOVA results for removal of sulfate by clinoptilolite.

Source	Sum of squares	Df	Mean square	F value	P value	Remarks
Model	5666.64	5	1133.33	16.47	0.004	Significant
A (pH)	3160.13	1	3160.13	45.92	0.0011	
B (D/C)	1696.13	1	1696.73	24.65	0.0042	
AB	222.01	1	222.01	3.23	0.0133	
A ²	548.59	1	548.59	7.97	0.0370	
Residual	344.11	5	68.82			
Lack of fit	344.11	3	114.7		0.2043	Not significant
Net error	0	2	0			
Total	6010.75	10				

Table 3 contains pH and D/C points, in which the optimal removal percentage occurred for clinoptilolite. As it is seen, these points for clinoptilolite are pH= 9.51 and D/C= 18.91. Using the data from Table 3, graphs of the effect of pH and D/C on adsorption of sulfate by clinoptilolite were mapped in Figs. 9 and 10. As shown in Fig. 9, the amount of adsorption of sulfate in the acidic region is less than that of the alkaline region. Also, it is precisely found in Fig. 10 that the amount of adsorption of sulfate by increasing the amount of adsorbent in the selected range by clinoptilolite has been reduced; but not very significantly.

Table 3. Results of validation of final optimal point in the multi-response optimization for clinoptilolite.

pH	D/C	Removal, %	Desirability
9.51	18.91	86.4979	0.915 Selected
10.31	18.91	85.866	0.907

3.3. Desorption of the adsorbent

Desorption is used to remove the nanoparticles from the solution and retest with a spectrophotometer to determine the amount of residual pollutant after applying the adsorbent. Filtration method was applied by using 10 nm Whatman filter paper 42 to dissolve the adsorbed clinoptilolite.

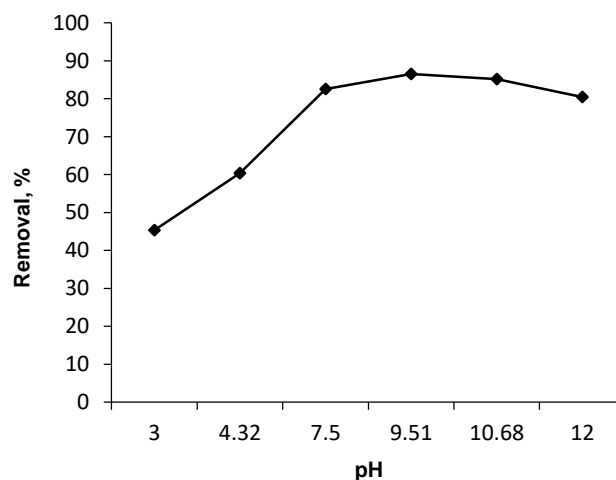


Fig. 9. Effect of pH on sulfate removal percentage by clinoptilolite.

3.4. Adsorption isotherm

Langmuir and Freundlich isotherms were calculated for clinoptilolite. Results are presented in Figs. 11 and 12. As it is shown,

Langmuir isotherm did not fit into the process of adsorbing sulfate by clinoptilolite. The correlation coefficient of the graph with the experimental data was 0.794 and theoretical adsorption capacity of sulfate was 74.63 mg/g. The R_L coefficient for this pollutant was 0.213, which, because it is between zero and one, is another confirmation for

the ion absorption process. On the other hand, the Freundlich isotherm well described the process of adsorbing sulfate by clinoptilolite. Its correlation coefficient was 0.918 and $1/n$ coefficient was equal to 0.1195.

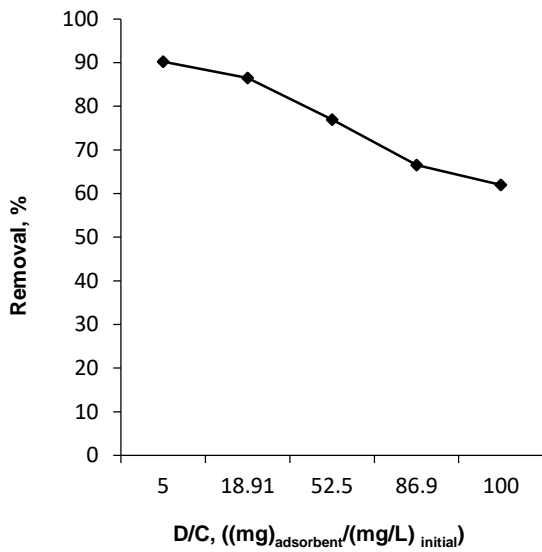


Fig. 10. Effect of D/C on the sulfate removal percentage by clinoptilolite.

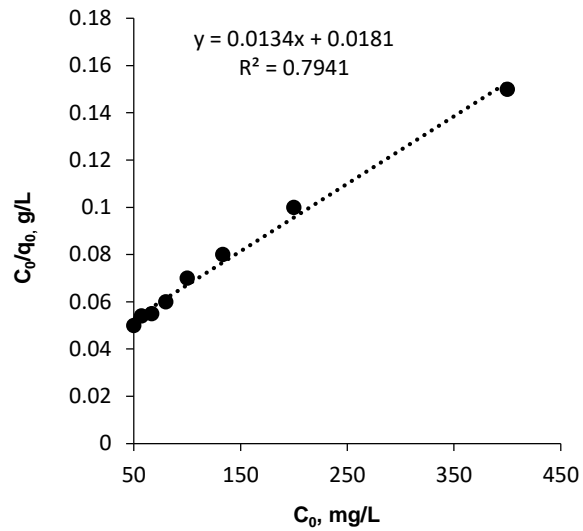


Fig. 11. Langmuir adsorption isotherm for sulfate by clinoptilolite.

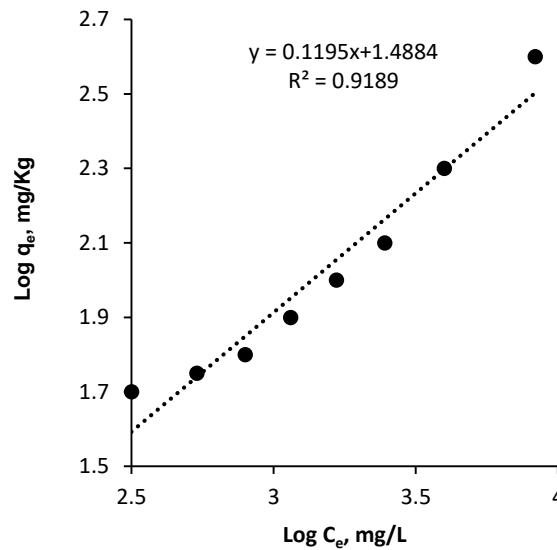


Fig. 12. Freundlich adsorption isotherm for sulfate by clinoptilolite.

4. Conclusions

In this study, nanoparticles of natural clinoptilolite were used to adsorb sulfate ions from Gamasiab river water samples. This long river flows thru Kermanshah city, Iran. Also, using experimental design and change in pH and adsorbent to contaminant ratio (D/C), it was attempted to determine the adsorption efficiency by clinoptilolite at 25 °C, 24-hour equilibrium and D/C ratio of 0-100. The best obtained removal efficiency was 91.5 %. Considering this efficiency, the measured amounts of sulfate, as well as the D/C ratio, were designed

to be tested. Results showed that optimum adsorption point for clinoptilolite was pH of 9.51 and D/C of 18.91, which resulted in an adsorption percentage of 86.5 in water samples.

Acknowledgement

We acknowledge the support of Kermanshah Regional Water Authority, Semnan University, Qom University, and Mr. Ali Shamshiri for this research.

References

- Alimohammadi V., Sedighi M., Jabbari E., Experimental study on efficient removal of total iron from wastewater using magnetic-modified multi-walled carbon nanotubes, Ecological Engineering 102 (2017) 90-97.
- Alimohammadi V., Sedighi M., Jabbari. E., Response surface modeling and optimization of nitrate removal from aqueous solutions using magnetic multi-walled carbon nanotubes. Journal of Environmental Chemical Engineering 4 (2016) 4525-4535.

- APHA, Standard methods for the examination of water and wastewater, 18th Edition, Denver: AWWA (1998).
- Biswas A.K., Water resources: Environmental planning, management and development. New York: McGraw-Hill (1997).
- Box G.E.P., Draper N.R., Response surfaces, mixtures, and ridge analyses. New Jersey: John Wiley & Sons, (2007).
- Devatha C., Thalla A.K., Katte S.Y., Green synthesis of iron nanoparticles using different leaf extracts for treatment of domestic waste water, *Journal of Cleaner Production* 139 (2016) 1425-1435.
- Ezzeddine Z., Batonneau-Gener I., Pouilloux Y., Hamad H., Saad Z., Kazpard V., Divalent heavy metals adsorption onto different types of EDTA-modified mesoporous materials: Effectiveness and complexation rate, *Microporous and Mesoporous Materials* 212 (2015) 125-136.
- Heizer W.D., Sandler R.S., Seal Jr E., Murray S.C., Busby M.G., Schliebe B.G., Pusek, S.N., Intestinal effects of sulfate in drinking water on normal human subjects, *Digestive Diseases and Sciences* 42 (1997) 1055-1061.
- Ho Y.S., Selection of optimum sorption isotherm, *Carbon* 42 (2004) 2115-2116.
- ISO B.S., Water quality-sampling-part 5: Guidance on sampling of drinking water from treatment works and piped distribution systems, London: British Standards Institution, (1991).
- Li Q., Zhan Z., Jin S., Tan B., Wetttable magnetic hypercrosslinked microporous nanoparticle as an efficient adsorbent for water treatment, *Chemical Engineering Journal* 326 (2017) 109-116.
- Ma Z., Shan C., Liang J., Tong M., Efficient adsorption of selenium (IV) from water by hematite modified magnetic nanoparticles. *Chemosphere* 193 (2018) 134-141.
- Montgomery D.C., Design and analysis of experiments. 6th Edition, with Design Expert Software, New Jersey: John Wiley & Sons (2004).
- Qu X., Alvarez P.J.J., Li Q., Applications of nanotechnology in water and wastewater treatment, *Water Research* 47 (2013) 3931-3946.
- Redlich O.J.D.L., Peterson D.L., A useful adsorption isotherm, *Journal of Physical Chemistry* 63 (1959) 1024-1034.
- Rabo J.A., Zeolite chemistry and catalysis, American Chemical Society 171 (1976) 25-46.
- Salimi A.H., Karami H., Farzin S., Hassanvand M.R., Azad A., Kisi O., Design of water supply system from rivers using artificial intelligence to model water hammer, *ISH Journal of Hydraulic Engineering* (2018) 1-10.
- Tao W., Chen G., Zeng G., Yan M., Chen A., Guo Z., Wang L., Influence of silver nanoparticles on heavy metals of pore water in contaminated river sediments, *Chemosphere* 162 (2016) 117-124.
- Zhao J., Dehbari N., Han W., Huang L., Tang Y., Electrospun multi-scale hybrid nanofiber/net with enhanced water swelling ability in rubber composites, *Materials & Design* 86 (2015) 14-21.